JPET Fast Forward. Published on November 10, 2006 as DOI:10.1124/jpet.106.114330

The novel γ secretase inhibitor MRK-560 reduces amyloid plaque deposition without evidence of Notch-related pathology in the Tg2576 mouse.

Authors: Jonathan D. Best, David W. Smith, Michael A. Reilly, Ruth O'Donnell, Huw D. Lewis, Semantha Ellis, Neil Wilkie, Thomas W. Rosahl, Philippe A. Laroque, Christine Boussiquet-Leroux, Ian Churcher, John R. Atack, Timothy Harrison, and Mark S. Shearman.

Department of In Vivo Neuroscience (J.D.B., J.R.A.), Department of Molecular & Cellular Neuroscience (D.W.S., R.O., H.D.W., S.E., N.W., T.W.R., M.S.S.), Department of Chemistry (M.A.R., I.C., T.H.), Merck Sharp & Dohme, Neuroscience Research Centre, Eastwick Road, Harlow, Essex, CM20 2QR, UK. Department of Safety Assessment (C.B-L, P.A.L) Merck Sharp & Dohme Research Centre, Chibret, Route de Marsat, Riom, 63963 Clermont-Ferrand, France

Copyright 2006 by the American Society for Pharmacology and Experimental Therapeutics.

a) Aβ plaque reduction without peripheral pathology.

b) Corresponding author: Jonathan Best.

Current address: DanioLabs Ltd.,

Unit 7330, Cambridge Research Park,

Waterbeach, Cambs., CB5 9TN, UK.

E-mail: jonathan.best@daniolabs.com

Tel: 01223 706460. Fax: 01223 706461

c) Number of text pages: 20

Number of figures: 5

Number of tables: 0

Number of references: 40

Number of words in Abstract: 235

Number of words in Introduction: 601

Number of words in Discussion: 1431

d) Abbreviations: Aβ, β-amyloid peptides; AD, Alzheimer's disease; APP, amyloid precursor protein; DEA, diethylamine; GnHCl, guanidine hydrochloride.

e) Section: Neuropharmacology

Abstract

There is a substantial body of evidence indicating that β-amyloid peptides (Aβ) are critical factors in the onset and development of Alzheimer's disease (AD). One strategy for combating AD is to reduce or eliminate the production of Aβ through inhibition of the γ-secretase enzyme which cleaves Aβ from the amyloid precursor protein (APP). We demonstrate here that chronic treatment for 3 months with 3 mg/kg of the potent, orally bioavailable and brain penetrant γ-secretase inhibitor MRK-560 attenuates the appearance of amyloid plaques in the Tg2576 mouse. These reductions in plaques were also accompanied by a decrease in the level of reactive gliosis. The morphometric and histological measures agreed with biochemical analysis of Aβ(40) and (42) in the cortex. Interestingly, the volume of the plaques across treatment groups did not change indicating that reducing Aβ levels does not significantly alter deposit growth once initiated. Further, we demonstrate that these beneficial effects can be achieved without causing histopathological changes in the ileum, spleen or thymus as a consequence of blockade of the processing of alternative substrates, such as the Notch family of receptors. This indicates that in vivo a therapeutic window between these substrates seems possible - a key concern in the development of this approach to AD. An understanding of the mechanisms whereby MRK-560 shows differentiation between the APP and Notch proteolytic pathway of γ-secretase should provide the basis for the next generation of γ-secretase inhibitors.

Introduction

AD is a devastating disorder of the aged population. Current treatments offer at best modest efficacy, thus there is a need for a therapy able to alter the disease's pathophysiology (Hardy and Selkoe, 2002). The neuropathology consists of insoluble deposits of Aβ plaques, reactive gliosis and intracellular neurofibrillary tangles of hyperphosphorylated tau (for reviews see Price and Sisodia, 1998; Selkoe, 2000). However, the precise relationship between these events remains to be established (Mudher and Lovestone, 2002).

Aβ peptides containing 40 or 42 amino acids are produced by sequential cleavage of APP by β-secretase and then c-terminally by γ-secretase (Selkoe, 1999). The Aβ(42) peptide is highly amyloidogenic, driving amyloid fibril formation which is considered the primary agent for direct amyloid toxicity and plaque formation (Maggio et al., 1992; Jarrett et al., 1993). Mutations in human APP around these secretase cleavage sites are associated with early-onset Familial AD, characterised by elevated levels of Aβ(42) (Price and Sisodia, 1998). Transgenic mice with mutant human APP demonstrate elevated production of Aβ(42), recapitulating the cerebral amyloidosis seen in AD (Games et al., 1995; Hsiao et al., 1996).

The amyloid deposition in these mouse brains is age-dependent, appearing slightly later than reported cognitive deficits (Janus and Westaway, 2001; Kawarabayashi et al., 2001; Lewis et al., 2004). Recently, a triple transgenic mouse revealed that the intracellular accumulation of the Aβ(42) peptide precedes extracellular plaque formation, correlating significantly with both the cognitive and electrophysiological dysfunction,

which further implicates Aβ(42) as a key pathological event in this disease (Oddo et al., 2003). Consequently, much effort has focused on the inhibition of Aβ production, with one strategy being to inhibit γ-secretase, an enzyme complex composed of presenilin, nicastrin, APH-1 and PEN-2 (reviewed in Haass, 2004). The development of selective γ-secretase inhibitors has allowed pharmacological reduction in Aβ production (for review see Harrison et al., 2004).

γ-secretase is a member of the I-CLiP protease family and cleaves a number of additional intramembrane substrates including CD-44, Erb4, E-cadherin, Notch and the Notch ligands Delta and Jagged 2 (for review see Wolfe and Kopan, 2004). One of the best characterised is the transmembrane protein Notch which is cleaved to become the transcriptionally active Notch Intracellular Domain (Hartmann et al., 2001; Wolfe and Kopan, 2004). Inhibition of its production has been identified as a potential concern for γ-secretase inhibitor therapy, as high levels of γ-secretase inhibition affect B and T cell maturation and ileal goblet cell formation (Searfoss et al., 2003; Wong et al., 2004).

Numerous studies have also demonstrated that Aβ is transported in and out of the brain by different mechanisms (for review see Zlokovic, 2004). Determining in vivo changes of Aβ and amyloid deposition in the central nervous system resulting from chronic γ-secretase inhibition will further aid our understanding of these dynamics.

Previously, we characterised the effects of the novel potent, bioavailable γ-secretase inhibitor MRK-560 (N-[cis-4-[(4-chlorophenyl)sulfonyl]-4- (2,5-difluorophenyl)cyclohexyl]-1,1,1- trifluoromethanesulfonamide, Churcher et al., 2006) on DEA-soluble Aβ in the brain and CSF of the rat, demonstrating a dose-dependent

effect on inhibition of Aβ production with a half-life suitable for once-a-day dosing. In addition, preliminary visual inspection of the gastrointestinal system in a two week dosing study of MRK-560 in the rat revealed no overt signs of toxicity (Best et al., 2006).

Thus, this study set out to determine the effect of chronic dosing of MRK-560 on Aβ levels and amyloid plaque formation in the Tg2576 mouse model of amyloid deposition. Secondly, we examined peripheral tissues histologically for signs of toxicity which may be related to altered Notch signaling (Doerfler et al., 2001; Hadland et al., 2001; Searfoss et al., 2003; Wong et al., 2004).

Materials and Methods

Animals and dosing. All procedures were conducted in accordance with the Animals (Scientific Procedures) Act of 1986 and its associated guidelines. Tg2576 transgenic mice (male and female) over-expressing human APP harbouring the Swedish mutation (K670N, M671L; Hsiao et al., 1996) were bred in-house. All animals were maintained on a 12:12 light:dark cycle with unrestricted access to food and water until use. Four month old mice were dosed orally for one week once a day with 3mg/kg of MRK-560 as a suspension in 0.5% methylcellulose at 10ml/kg. For the chronic study, 12 month old mice were dosed orally for 3 months once a day with 3mg/kg of MRK-560 as a suspension in 0.5% methylcellulose at 10ml/kg.

Tissue sample preparation for one week study. Tg2576 mice were euthanased by stunning followed by decapitation at predetermined time points. Brains were removed, immediately frozen on dry ice and stored at -80°C until use. The frozen brains were

homogenized in 10 volumes (w:v) of 0.2% diethylamine (DEA) containing 50mM NaCl (pH 10) and protease inhibitors (Complete™, Roche, Mannheim, Germany) (Savage et al., 1998), then centrifuged at 355,000*g*, 4°C, for 30min (Beckman Coulter Ultra Centrifuge, Optima Max, Fullerton, CA). The resulting supernatant was retained as the soluble fraction and neutralized by addition of 10% 0.5M TrisHCl, pH 6.8. Samples were frozen at -80°C awaiting analysis by immunoassay (in young plaque-free mice DEA-extraction yields similar levels of Aβ to the guanidine hydrochloride (GnHCl) method; Best et al., 2005).

Necropsy and tissue collection after chronic dosing study. At necropsy the brain was removed and divided into four quadrants. The frontal two quadrants, extending from the optic chiasm rostrally and including the frontal cortex, striatum and olfactory bulbs, were frozen on dry ice. The remaining two caudal quadrants containing the hippocampus, overlying cortex, cerebellum and brainstem were separated along the midline. The left hemisphere was frozen in isopentane held at -40°C on dry ice and then stored at -80°C. The remaining right caudal quadrant was immersion fixed in 10% neutral buffered formalin and processed in paraffin wax for serial sectioning in the sagittal plane. All remaining organs were dissected and immersion fixed in 10% neutral buffered formalin; selected organs were further processed and sectioned for subsequent analysis.

Immunoassay analysis. The protocol used for extraction of 'total' amyloid from the brain sections is based on the GnHCl extraction method described elsewhere (Johnson-Wood et al., 1997). The frontal brain quadrants were homogenised in 10 volumes of 5M GnHCl, 50mM HEPES (pH 7.3), 5mM EDTA plus 1X EDTA–free protease inhibitor cocktail (Complete™). Following mixing at room temperature for 3 hours, the

homogenate was diluted ten-fold into ice-cold 25mM HEPES (pH 7.3), 1mM EDTA, 0.1% BSA plus 1X protease inhibitor cocktail and centrifuged at 16,000*g* for 20min at 4^{o}C. Aliquots of supernatant were stored at –80^{o}C to prevent degradation. The biotinylated antibody 4G8 (Kim et al., 1988) was used in combination with the monoclonal antibodies G2-10 or G2-11 for detection of Aβ(40) or Aβ(42) respectively (Ida et al., 1996). These species reflect subpopulations of peptides with heterogeneous N-termini encompassing at least the 4G8 epitope at residues 17-24. Analysis of the samples was performed using the Meso Scale Discovery Sector Imager 6000 (Gaithersburg, MD), as described elsewhere (Best et al., 2005).

Immunohistochemistry. A uniform random sample of sections representing 10 levels from the dorsomedial extent of the right caudal quadrant was selected for immunohistochemical labeling. Briefly, sections were dewaxed and rehydrated through graded alcohols to phosphate buffered saline. Immunohistochemical staining was performed in accordance with the manufacturer's instructions using the anti-mouse IgG Vectastain Elite ABC kit and Mouse on Mouse blocking reagents (Vector Laboratories, Peterborough, UK). Aβ(40) was labelled using a mouse monoclonal antibody G2-10 at a dilution of 1:300. Sections were counterstained in Gill's haematoxylin (A. Menarini Diagnostics, High Wycombe, UK), dehydrated, cleared and mounted.

Ligand autoradiography. A frozen quadrant of brain containing the hippocampus was serial sectioned at 20μm in the sagittal plan; three sections per slide were taken onto sterile SuperFrost Plus and the next three sections discarded. A uniform random sample (sections taken at a uniform interval to give twelve levels per animal) was taken for

radiolabeled amyloid binding using a modified version of the protocol used by Maggio et al. (1992). The slides generated from the sectioning procedure were stored at –80^{o}C until required. Sections were brought to room temperature and pre-incubated in 50mM Tris (pH 7.4), 10mM $MnCl_2$, 0.004% bacitracin, 0.002% chymostatin and 0.004% leupeptin for 10min prior to addition of radioligand at 50pM (25µCi; GE Healthcare Life Sciences, Buckinghamshire, UK). After incubation with the radioligand for two hours, the slides were washed with 50mM Tris HCl (pH 7.4; four 2-min washes at 4^{o}C) and distilled water. The slides were then allowed to dry at room temperature. The fully dried slides were apposed to film (Kodak Biomax MR, Kodak Ltd, Hemel Hempstead, UK) along with radio-iodinated standards for 7 days (GE Healthcare Life Sciences). All films contained representatives of each treatment group to ensure standardization across the study. The film images for each group were captured and analysed for plaque numbers digitally (Microdensitometry-based Computer-assisted Imaging Device (MCID)-Analytical Imaging Station (AIS) 6.0, Imaging Research Inc., ON, Canada). The mean plaque or "deposit" volume was calculated by dividing the stereologically derived total amyloid volume by the total number of plaques.

Histopathology. 6µm haematoxylin- and eosin-stained sections of brain at 5 representative levels, and sections of ileum, spleen and thymus, were examined by a blinded skilled pathologist for the qualitative evaluation of any treatment related changes.

Western blotting. Brains from control and compound-treated Tg2576 mice were weighed and lysed in 15 volumes of ice-cold lysis buffer (20mM Tris (pH 7.4), 150mM NaCl, 1mM EDTA, 1mM EGTA, 1% Triton, 2.5mM sodium pyrophosphate, 1mM β-

glycerophosphate, 1mM sodium orthovanadate, 1μg/ml leupeptin, 1mM 4-(2-aminoethyl)-bezenesulfonylfluoride) using a Teflon-coated pestle and mortar. Insoluble material was removed via centrifugation at 14,000rpm for 5min. The resulting supernatant was assayed for total protein content using the BCA microprotein assay (Perbio Science UK Ltd., Cramlington, UK), mixed 1:1 with 2X sample buffer and 30μg was loaded per well onto 26-well 10% BisTris XT gels (Bio-Rad, Hemel Hempstead, UK). Electrophoresed proteins were transferred to Protran nitrocellulose membranes (Schleicher & Schuell, Dassel/Relliehausen, Germany). Primary immunodetection was via anti-glial fibrillary acidic protein (GFAP) (1:1000, Dako, Ely, UK); specific bands were visualised using IR Dye-conjugated secondary antibodies and quantified using the Odyssey infra-red imager (LI-COR Biosciences UK Ltd., Cambridge, UK).

Results

One week dosing study of MRK-560 in young Tg2576 mice. Based on previous measurements of the pharmacokinetic properties of MRK-560 (Best et al., 2006) and efficacy achieved in APP-YAC mice, (Churcher et al., 2006) 3mg/kg was administered *p.o*. to Tg2576 mice for one week (steady state level) to determine the reduction of DEA-soluble brain Aβ(40) levels in order to establish reduction of Aβ for the chronic studies (fig 1). As expected the reduction of these soluble Aβ(40) levels was fairly constant during the time course, with the integrated reduction over 24h being 79%. Since in young plaque-free mice DEA-extracted Aβ should equate to GnHCl-extracted Aβ (Best et al., 2005), this dose of 3mg/kg was chosen for chronic (3 month) dosing.

Effect of chronic administration of MRK-560 on Aβ levels in aged Tg2576 mice. Animals were dosed from 12 months of age for 3 months. Chronic administration of 3mg/kg/day of MRK-560 did not lead to either increased mortality or deviation from control values for weight during the study period (data not shown). Initial levels of GnHCl-extracted Aβ(40) and (42) at 12 months of age were 1.47 $\pm$ 0.25 and 0.54 $\pm$ 0.07nmol/g respectively.

After 3 months of dosing, the levels of Aβ(40) in this 15 month old group of animals receiving vehicle had increased to 9.63 $\pm$ 0.95nmol/mg (fig 2A), an increase of approximately 6-7 fold compared to the 12 month old animals. The animals receiving 3mg/kg of MRK-560 had levels of Aβ(40) of 5.48 $\pm$ 0.10nmol/mg. This was a significant reduction of 43% compared to the 15 month vehicle group (student's t-test, $p<0.01$). The levels of Aβ(42) (fig 2B) in the vehicle group were 3.90 $\pm$ 0.423nmol/mg, also an

increase of approximately 7 fold compared to the 12 month old animals. In the group receiving 3mg/kg of MRK-560 the levels of Aβ(42) were 2.22 ± 0.22nmol/mg. This was also equivalent to a 43% reduction compared to the 15 month old vehicle group (student's t-test, $p<0.01$).

Effect of chronic administration of MRK-560 on plaque numbers in aged Tg2576 mice. Evaluation of autoradiographic sections from the frozen caudal brain quadrant labelled with ^{125}I Aβ(1-40) revealed a substantial decrease in the amount of binding in the inhibitor-treated versus vehicle-treated animals (fig 3A vs B). Quantification of this binding demonstrated a significant 49% decrease in the number of amyloid deposits to which the ^{125}I Aβ(1-40) was bound (fig 3C; student's t-test, $p<0.01$). There was no significant change in the average volume of deposits when compared across groups (fig 3D). This was derived by dividing the total amyloid volume by the deposit number. To confirm the effect seen with the ^{125}I Aβ labeling, paraformaldehyde-fixed paraffin-embedded sections were immunolabelled for Aβ(40) using the N-terminus G2-10 antibody. The immunoreactivity also revealed a similar decrease in the number of plaque deposits in the γ-secretase inhibitor-dosed group (fig 3E vs F).

Effect of MRK-560 on associated gliosis in aged Tg2576 mice. Reactive astrocytosis is known to be associated with an increase in Aβ levels in AD. To determine if this relationship was maintained in this study, western blot analysis was performed for GFAP on the brains of the mice (fig 4). The western blots demonstrated a decrease in the levels of GFAP in response to the inhibitor. When the blots were quantified a significant decrease of 27% was observed (student's t-test, $p<0.05$).

Histopathology after chronic administration of MRK-560 in peripheral tissues of Tg2576 mice. One of the main concerns regarding the use of γ-secretase inhibitors is the off-target effects on substrates and organs not directly related to the neuropathology of AD (Searfoss et al., 2003; Wong et al., 2004). Of these, the ileum, thymus and spleen have been picked out as potential targets and markers of this side effect liability. To determine if there were any off-target effects caused by this dosing regime, sections of ileum (fig 5A, B), spleen (fig 5C, D) and thymus (fig 5E, F) were examined for any microscopic changes relating to the administration of MRK-560. There were no discernable differences between any of these tissue sections; in the case of the ileum this was particularly related to the number of goblet cells which did not change along with the tissue architecture. The same picture was seen in the thymus and spleen. In the spleen, there was no discernable decrease in the size of the marginal zone cells (lighter staining; fig 5C and D) between the vehicle and MRK-560 group. In the thymus, the expected atrophy of the cortical zone was not seen, with a clear demarcation between the darker stained cortical zone and lighter stained medullary zone seen in both vehicle and MRK-560 groups (fig 5E and F). Microscopically, although the number of cells was not quantified, no morphological differences were seen between cells from the vehicle and the MRK-560 groups of animals in either the spleen or thymus. These findings indicated no deleterious effects of MRK-560 on the cell differentiation pathways in these peripheral tissues.

Discussion

The ability of γ-secretase inhibitors to lower levels of Aβ after acute *in vitro* and *in vivo* exposure has been reported in various model systems (for review see Churcher and Beher, 2005). There are also reports investigating the effects of these types of compounds on Aβ in old transgenic mice following chronic administration (Barten et al., 2005). Our data represent the first demonstration that chronic administration of a γ-secretase inhibitor during a period of accelerated plaque deposition can significantly reduce the initiation and extent of these lesions without significant effects on the peripheral tissues.

Using a combined approach of biochemical and histological analysis, we have demonstrated a significant decrease in both the number and extent of amyloid deposits in the cortex of inhibitor-treated mice when compared with their vehicle-treated controls. These differences were significant in all three assay systems. Immunohistochemical and ^{125}I Aβ detection of plaques revealed a significant decrease in the overall fraction occupied by amyloid.

Interestingly, individual deposits in treated mice did not differ in average size from those seen in equivalent vehicle-dosed animals. This would imply that reduction of Aβ by 40-50% has a significant effect on the initiation of the formation of plaques rather than their growth or clearance. Hence, it is likely that once seeded, amyloid concentrations remain sufficient for plaques to increase in size at a rate similar to that seen under control conditions. This may be especially true in the presence of lower overall numbers of deposits acting as a sink for the soluble amyloid pool. Recent reports have demonstrated that intracellular accumulation of Aβ(1-42) can precede the appearance of extracellular

plaques (Oddo et al., 2003) and that dense aggregates of Aβ(1-42), considered to be the focus for further deposition, are deposited prior to the appearance of diffuse amyloid. Given the clear reduction in plaque-deposited Aβ40 it would also be interesting to use thioflavin staining and immunohistochemical staining for Aβ42 to determine whether dense core plaques numbers are affected differently by MRK-560 treatment. Thus, taking these observations into account, sustained γ-secretase inhibition during a period when the accumulation and aggregation of intraneuronal amyloid is causing cellular and synaptic degeneration may be critical.

Previously we have established that GnHCl extraction (Lewis et al., 2004; Johnson-Wood et al., 1997) of brain homogenates extracted a significant proportion of the total amyloid pool in this mouse model. This extraction protocol solubilises most of the amyloid except some plaque core and vascular amyloid (unpublished observation, DS). At 15 months, the soluble pool (as reflected by sodium dodecyl sulphate or DEA extraction) makes up about 10% of the Aβ pool extracted by formic acid or GnHCl (Kawarabayashi et al., 2001). The lowering in plaque number as assessed by ^{125}I labeling agreed well with the decrease in GnHCl-extracted Aβ for both Aβ(40) and Aβ(42) in the sampled brain containing the olfactory bulb, frontal cortex and striatum suggesting that these biochemical measures are an accurate reflection of overall amyloid load including plaque number.

Plaque formation and maturation are normally accompanied by inflammatory processes. Initial findings using western blot analysis to assess GFAP immunoreactivity demonstrated a reduction in the Tg2576 mice chronically treated with the γ-secretase

inhibitor. Since these reductions probably reflect the decrease in the number of lesions rather than a generalised decrease in the activation of glia, detailed immunohistochemistry with morphological evaluation and quantification would be required as there is no evidence that an individual deposit, once formed does not elicit the typical glial response and subsequent damage to the surrounding neuropil.

A key to establishing the clinical viability of γ-secretase inhibition is the demonstration of a safety window between the effects on processing of APP and the effect on alternative substrates for γ-secretase, particularly the Notch family of receptors. It has been suggested that this lack of substrate specificity has the potential to lead to adverse effects.

Much is known about the developmental importance of Notch in cell fate determination. Removal of the Notch pathway transcription factor CSL/RBP-J in transgenic mice generated defects in the gastrointestinal tract with a similar phenotype being achieved using the γ-secretase inhibitor dibenzazepine (DBZ) (van Es et al., 2005). This effect was also demonstrated in rats after 4-5 days of dosing with the γ-secretase inhibitors compound X and DBZ (Searfoss et al., 2003; Milano et al., 2004). The effects manifested themselves grossly as an increase in the gastrointestinal weight associated with distension of the small and large intestines. Microscopically, goblet cell metaplasia was observed in the ileal lumen along with abnormal villus architecture. Another organ affected was the spleen, where a decrease in the number of marginal zone cells was observed. In TgCRND8 mice dosed with the γ-secretase inhibitor LY-411575 for 2

weeks, atrophy of the thymus was reported with doses which gave between 60-80% reduction of Aβ(40) and (42) (Wong et al., 2004).

Recently, a number of reports have revealed compounds that can distinguish between the proteolytic activities of APP and Notch. These compounds are not classical γ-secretase inhibitors (i.e. they do not inhibit the production of Aβ(1-40) and Aβ(1-42) equally); rather they are modulators of γ-secretase cleavage specificity in that they favour the reduction of Aβ(42) production. Such compounds include a subset of NSAIDs which preferentially reduced Aβ(42) production without appearing to affect Aβ(40) or Notch processing (Weggen et al., 2001, 2003). However, evidence is contradictory as to whether these compounds are effective *in vivo* (Lanz et al., 2005; Eriksen et al., 2003). Similarly, of the pan inhibitors, the arylsufonamide BMS-299897 appeared to have a 15 fold separation between APP and Notch processing in HEK293 cells (Barten et al., 2005). *In vivo*, separate studies in rats and Tg2576 mice revealed there were no adverse phenotypes in gut, spleen or thymus when BMS-299897 was dosed for a period between 5 days and 2 weeks (Barten et al., 2005; Milano et al., 2004). However, brain Aβ reduction was not investigated in the rats and BMS-299897 was unable to lower brain Aβ(40) in the aged plaque-bearing Tg2576 mice (Barten et al., 2005). Thus in these studies no window between amyloid production and Notch cleavage has been unequivocally demonstrated *in vivo*.

We conducted detailed histopathological evaluation of a number of potential target organs in the mice which had been treated for 3 months. Analysis of the gastrointestinal tract (represented by the ileum) revealed no gross changes in weight or appearance.

Microscopically, there were no differences in goblet cell numbers or general villus architecture between the vehicle-dosed animals and the animals receiving MRK-560. The spleen presented no change in the marginal cell zone between the groups; this is consistent with the previous data for BMS-299897. Finally, evaluation of the thymus demonstrated no atrophy or abnormal changes in contrast to the changes caused by LY-411575 in the TgCRND8 mice (Wong et al., 2004).

When taken together, our data demonstrate that chronic γ-secretase inhibition can significantly reduce the induction of amyloid deposits together with the associated inflammatory changes in the brains of Tg2576 mice. This can be achieved at levels of inhibition that do not appear to induce histopathological changes in the brain or peripheral organs which would be associated with inhibition of processing of alternative substrates by this enzyme complex.

In vitro, there appears to be little or no separation for MRK-560 between the inhibition of the APP and Notch processing pathway (Churcher et al., 2006). Using HEK293 cells stably coexpressing APP and NotchΔE (Lewis et al., 2003); MRK-560 had IC50 values for APP and Notch cleavage of 4.32nM and 3.44nM respectively. In this same assay LY-411575 gave values of 0.119nM for APP and 0.129nM for NotchΔE (Lewis et al., 2003). Since LY-411575 has been shown to cause severe peripheral organ toxicity in TgCRND8 mice (Wong et al., 2004), a full characterization of the therapeutic window of MRK-560 *in vivo* in this dosing paradigm is needed to be able to compare these inhibitors.

The mechanism whereby MRK-560 has beneficial effects on amyloid plaque deposition in the absence of toxicity related to changes in the Notch signaling pathway

remains to be elucidated. However, the composition of the γ-secretase complex can vary from tissue to tissue with respect to differences in the APH-1 isoforms (Serneels et al., 2005). This offers the intriguing possibility that certain structural classes of γ-secretase inhibitors may preferentially affect brain but not peripheral γ-secretase complexes. This idea could be further investigated using other endpoints such as HES expression (Milano et al., 2004). This would then refocus attention on γ-secretase inhibitors as a possible therapy for AD; an approach which until now appeared to be limited due to mechanism-based peripheral toxicity (Searfoss et al., 2003; Wong et al., 2004).

Acknowledgements: The authors are grateful to the following for their assistance, John R. Curry, James Peachey, Angela Jennings, Emma Armstrong, David Williamson, Graham Bentley, Richard Jennison, Teresa Mallia, Paul Mackin, Matt Clayton and the biological services team. Thank you to Julia Hunt for critical review of this manuscript.

References

Barten DM, Guss VL, Corsa JA, Loo A, Hansel SB, Zheng M, Munoz B, Srinivasan K, Wang B, Robertson BJ, Polson CT, Wang J, Roberts SB, Hendrick JP, Anderson JJ, Loy JK, Denton R, Verdoorn TA, Smith DW, Felsenstein KM. (2005) Dynamics of β-amyloid reductions in brain, cerebrospinal fluid, and plasma of β–amyloid precursor protein transgenic mice treated with a γ-secretase inhibitor. J Pharmacol Exp Ther 312:635-643.

Best JD, Jay MT, Otu F, Ma J, Nadin A, Ellis S, Lewis HD, Pattison C, Reilly M, Harrison T, Shearman MS, Williamson TL, Atack JR. (2005) Quantitative measurement of changes in amyloid-β(40) in the rat brain and cerebrospinal fluid following treatment with the γ-secretase inhibitor LY-411575 [N2-[(2S)-2-(3,5-difluorophenyl)-2-hydroxyethanoyl]-N1-[(7S)-5-methyl-6-oxo-6,7-dihydro-5H-dibenzo[b,d]azepin-7-yl]-L-alaninamide]. J Pharmacol Exp Ther 313:902-908.

Best JD, Jay MT, Otu F, Churcher I, Reilly M, Morentin-Gutierrez P, Pattison C, Harrison T, Shearman MS, Atack JR. (2006) In vivo characterization of Aβ(40) changes in brain and cerebrospinal fluid using the novel γ-secretase inhibitor N-[cis-4-[(4-chlorophenyl)sulfonyl]-4-(2,5-difluorophenyl)cyclohexyl]-1,1,1-trifluoromethanesulfonamide (MRK-560) in the rat. J Pharmacol Exp Ther 317:786-90.

Churcher I, Beher D. (2005) γ-secretase as a therapeutic target for the treatment of Alzheimer's disease. Curr Pharmaceutical Design 11:3363-3382.

Churcher I, Beher D, Best JD, Castro JL, Clarke EE, Gentry A, Harrison T, Hitzel L, Kay E, Kerrad S, Lewis HD, Morentin-Gutierrez P, Mortishire-Smith R, Oakley PJ, Reilly M, Shaw DE, Shearman MS, Teall MR, Williams S, Wrigley JD. (2006) 4-substituted cyclohexyl sulfones as potent, orally active γ-secretase inhibitors. Bioorg Med Chem Lett 16:280-284.

Doerfler P, Shearman MS, Perlmutter RM. (2001) Presenilin-dependent γ-secretase activity modulates thymocyte development. Proc Nat Acad Sci USA 98:9312-9317.

Eriksen JL, Sagi SA, Smith TE, Weggen S, Das P, McLendon DC, Ozols VV, Jessing KW, Zavitz KH, Koo EH, Golde TE. (2003) NSAIDs and enantiomers of flurbiprofen target γ-secretase and lower Aβ 42 in vivo. J Clin Invest 112:440-449.

Games D, Adams D, Alessandrini R, Barbour R, Berthelette P, Blackwell C, Carr T, Clemens J, Donaldson T, Gillespie F, Guido T, Hagopian S, Johnson-Wood K, Khan K, Lee M, Leibowitz P, Lieberburg I, Little S, Masliahparallel E, McConlogue L, Montoya-Zavala M, Muckestar L, Paganini L, Penniman E, Power M, Schenk D, Seubert P, Snyder B, Soriano F, Tan H, Vitale J, Wadsworth S, Wolozin B, Zhao J.

(1995) Alzheimer-type neuropathology in transgenic mice overexpressing V717F β-amyloid precursor protein. Nature 373:523-527.

Haass C. (2004) Take five- BACE and the γ-secretase quartet conduct Alzheimer's amyloid β-peptide generation. Embo J 23:483-488.

Hadland BK, Manley NR, Su D, Longmore GD, Moore CL, Wolfe MS, Schroeter EH, Kopan R. (2001) γ-secretase inhibitors repress thymocyte development. Proc Nat Acad Sci USA 98:7487-7491.

Hardy J, Selkoe DJ. (2002) The amyloid hypothesis of Alzheimer's disease: progress and problems on the road to therapeutics. Science 297:353-356.

Harrison T, Churcher I, Beher D. (2004) γ-secretase as a target for drug intervention in Alzheimer's disease. Curr Opin Drug Disc and Dev 7:709-719.

Hartmann D, Tournoy J, Saftig P, Annaert W, De Strooper B. (2001) Implication of APP secretases in notch signaling. J Mol Neurosci 17:171-181.

Hsiao K, Chapman P, Nilsen S, Eckman C, Harigaya Y, Younkin S, Yang F, Cole G. (1996) Correlative memory deficits, Aβ elevation, and amyloid plaques in transgenic mice. Science 274:99-102.

Ida N, Hartmann T, Pantel J, Schroder J, Zerfass R, Forstl H, Sandbrink R, Masters CL, and Beyreuther K (1996) Analysis of heterogeneous A4 peptides in human cerebrospinal fluid and blood by a newly developed sensitive Western blot assay. J Biol Chem 271:22908–22914.

Janus C, Westaway D. (2001) Transgenic mouse models of Alzheimer's disease. Physiol Behav 73:873-886.

Jarrett JT, Berger EP, Lansbury PT Jr. (1993) The carboxy terminus of the β amyloid protein is critical for the seeding of amyloid formation: implications for the pathogenesis of Alzheimer's disease. Biochem 32:4693-4697.

Johnson-Wood K, Lee M, Motter R, Hu K, Gordon G, Barbour R, Khan K, Gordon M, Tan H, Games D, Lieberburg I, Schenk D, Seubert P, McConlogue L. (1997) Amyloid precursor protein processing and A β42 deposition in a transgenic mouse model of Alzheimer disease. Proc Nat Acad Sci USA 94:1550-1555.

Kawarabayashi T, Younkin LH, Saido TC, Shoji M, Ashe KH, Younkin SG. (2001) Age-dependent changes in brain, CSF, and plasma amyloid (β) protein in the Tg2576 transgenic mouse model of Alzheimer's disease. J Neurosci 21:372-381.

Kim KS, Miller DL, Sapienza VJ, Chen C-MJ, Bai C, Grundke-Iqbal I, Currie JR, Wisniewski HM (1988) Production and characterization of monoclonal antibodies reactive to synthetic cerebrovascular amyloid peptide. Neurosci Res Commun 2:121–130.

Lanz TA, Fici GJ, Merchant KM. (2005) Lack of specific amyloid-β(1-42) suppression by nonsteroidal anti-inflammatory drugs in young, plaque-free Tg2576 mice and in guinea pig neuronal cultures. J Pharmacol Exp Ther 312: 399-406.

Lewis HD, Perez Revuelta BI, Nadin A, Neduvelil JG, Harrison T, Pollack SJ, Shearman MS. (2003) Catalytic site-directed gamma-secretase complex inhibitors do not discriminate pharmacologically between Notch S3 and beta-APP cleavages. Biochemistry 42:7580-7586.

Lewis HD, Beher D, Smith D, Hewson L, Cookson N, Reynolds DS, Dawson GR, Jiang M, Van der Ploeg LH, Qian S, Rosahl TW, Kalaria RN, Shearman MS. (2004) Novel aspects of accumulation dynamics and Aβ composition in transgenic models of AD. Neurobiol Aging 25:1175-1185.

Maggio JE, Stimson ER, Ghilardi JR, Allen CJ, Dahl CE, Whitcomb DC, Vigna SR, Vinters HV, Labenski ME, Mantyh PW. (1992) Reversible in vitro growth of

Alzheimer disease β-amyloid plaques by deposition of labeled amyloid peptide. Proc Nat Acad Sci USA 89:5462-5466.

Milano J, McKay J, Dagenais C, Foster-Brown L, Pognan F, Gadient R, Jacobs RT, Zacco A, Greenberg B, Ciaccio PJ. (2004) Modulation of notch processing by γ-secretase inhibitors causes intestinal goblet cell metaplasia and induction of genes known to specify gut secretory lineage differentiation. Toxicol Sci 82:341-358.

Mudher A, Lovestone S. (2002) Alzheimer's disease- do tauists and baptists finally shake hands? Trends Neurosci 25:22-26.

Oddo S, Caccamo A, Kitazawa M, Tseng BP, LaFerla FM. (2003) Amyloid deposition precedes tangle formation in a triple transgenic model of Alzheimer's disease. Neurobiol Aging 241063-1070.

Price DL, Sisodia SS. (1998) Mutant genes in familial Alzheimer's disease and transgenic models. Ann Rev Neurosci 21:479-505.

Savage MJ, Trusko SP, Howland DS, Pinsker LR, Mistretta S, Reaume AG, Greenberg BD, Siman R, Scott RW. (1998) Turnover of amyloid β-protein in mouse brain and acute reduction of its level by phorbol ester. J Neurosci 18:1743-1752.

Searfoss GH, Jordan WH, Calligaro DO, Galbreath EJ, Schirtzinger LM, Berridge BR, Gao H, Higgins MA, May PC, Ryan TP. (2003) Adipsin, a biomarker of gastrointestinal toxicity mediated by a functional γ-secretase inhibitor. J Biol Chem 278:46107-46116.

Selkoe DJ. (1999) Translating cell biology into therapeutic advances in Alzheimer's disease. Nature 399:A23-A31.

Selkoe DJ. (2000) Toward a comprehensive theory for Alzheimer's disease. Hypothesis: Alzheimer's disease is caused by the cerebral accumulation and cytotoxicity of amyloid β-protein. Ann N Y Acad Sci 924:17-25.

Selkoe DJ, Schenk D. (2003) Alzheimer's disease: molecular understanding predicts amyloid-based therapeutics. Ann Rev Pharmacol Toxicol 43:545-584.

Serneels L, Dejaegere T, Craessaerts K, Horre K, Jorissen E, Tousseyn T, Hebert S, Coolen M, Martens G, Zwijsen A, Annaert W, Hartmann D, De Strooper B. (2005) Differential contribution of the three Aph1 genes to γ-secretase activity in vivo. Proc Nat Acad Sci USA 102:1719-1724.

van Es JH, van Gijn ME, Riccio O, van den Born M, Vooijs M, Begthel H, Cozijnsen M, Robine S, Winton DJ, Radtke F, Clevers H. (2005) Notch/γ-secretase inhibition turns

proliferative cells in intestinal crypts and adenomas into goblet cells. Nature 435:959-963.

Weggen S, Eriksen JL, Das P, Sagi SA, Wang R, Pietrzik CU, Findlay KA, Smith TE, Murphy MP, Bulter T, Kang DE, Marquez-Sterling N, Golde TE, Koo EH. (2001) A subset of NSAIDs lower amyloidogenic Aβ42 independently of cyclooxygenase activity. Nature 414:212-216.

Weggen S, Eriksen JL, Sagi SA, Pietrzik CU, Ozols V, Fauq A, Golde TE, Koo EH. (2003) Evidence that nonsteroidal anti-inflammatory drugs decrease amyloid β 42 production by direct modulation of γ-secretase activity. J Biol Chem 278:30748-30754.

Wolfe MS, Kopan R. (2004) Intramembrane proteolysis: themes and variations. Science 305, 1119-1123.

Wong GT, Manfra D, Poulet FM, Zhang Q, Josien H, Bara T, Engstrom L, Pinzon-Ortiz M, Fine JS, Lee HJ, Zhang L, Higgins GA, Parker EM. (2004) Chronic treatment with the γ-secretase inhibitor LY-411,575 inhibits β-amyloid peptide production and alters lymphopoiesis and intestinal cell differentiation. J Biol Chem 279:12876-12882.

Zlokovic BV (2004) Clearing amyloid through the blood-brain barrier. J Neurochem 89:807-811

Footnotes

JDB and DWS contributed equally to this publication.

Current addresses for the following authors.

DWS: Dept of Neuroscience, Amgen, 1 Amgen Centre Drive, Thousand Oaks, CA 91320 USA

MAR: WP75B-200, Merck & Co. Inc., 770 Sumneytown Pike, P.O. Box 4, West Point, PA 19486, USA

HDL: Neurology & GI CEDD, GlaxoSmithKline Pharmaceuticals, New Frontiers Science Park, Third Avenue, Harlow, Essex CM19 5AW, UK

SE: Cellzome (UK) Ltd. Chesterford Research Park, Little Chesterford, Cambridge, CB10 1XL, UK.

NW: ITI Life Sciences, Innovation House, 17 Luna Place, Dundee Technology Park, Dundee, Scotland, DD2 1TP

TWR: Department of Molecular Profiling, Merck Research Laboratories, Merck & Co, Inc., RY80Y-310, PO Box 2000, Rahway, NJ, 07065, USA

IC: Dept of Medicinal Chemistry, Molecular Discovery Research, GlaxoSmithKline Medicines Research Centre, Gunnels Wood Road, Stevenage, SG1 2NY, UK.

JRA: Johnson & Johnson PR&D, 3210 Merryfield Row, La Jolla, San Diego CA 92121, USA

TH: Research & Development, Almac Sciences, 20, Seagoe Industrial Estate, Craigavon, BT63 5QD, Northern Ireland, UK.

MSS: Neuroscience Drug Discovery Merck Research Laboratories Boston, 33 Avenue Louis Pasteur, Boston MA 02115, USA.

Legends for Figures

Figure 1. Steady state levels of MRK-560 after once a day dosing for seven days reduce Aβ(40) levels for 24h in Tg2576 mice. Time course graph of the effect of 3mg/kg (●) of MRK-560 on DEA-extracted Aβ(40) levels in the brain. Animals were culled immediately 4, 8, 16 or 24 h after the last dose. Data points represent average Aβ(40) levels normalised to the vehicle levels ± SEM (n=3-5/data point).

Figure 2. Chronic dosing of 3mg/kg MRK-560 once a day for three months reduces total Aβ levels in the brains of Tg2576 mice. Graphs represent effects of vehicle (clear bars) vs 3mg/kg of MRK-560 (shaded bar) on GnHCl-extracted A) Aβ(40) levels and B) Aβ(42) levels. Columns represent average Aβ levels (nmol/g ± SEM, n=22-23 per column). ** represents $p<0.01$.

Figure 3. Plaque burden is reduced in the brains of Tg2576 mice treated with 3mg/kg MRK-560 once a day for three months. Autoradiographs of posterior quadrants of the brain including areas such as cortex, hippocampus and cerebellum for the radioligand binding of ^{125}I Aβ to plaques in mice treated with either A) vehicle or B) MRK-560. Note main localization of binding to cortex and hippocampal areas and marked reduction of binding in MRK-560 group. C) Quantification of binding (expressed as number of plaques per mm^3 of cortex) demonstrating a significant reduction in the MRK-560-treated group ($p<0.01$) (n=12). D) Quantification of the mean deposit volume showing that there was no overall difference in the size of the plaques between the vehicle and MRK-560

group (n=12). Immunohistochemical labeling of plaques with G2-10 antibody in the cortex and hippocampus in the E) vehicle- and F) MRK-560-dosed group revealing a reduction in the number of plaques in the MRK-560-treated group. Inset shows close up labeled plaque.

Figure 4. GFAP staining is reduced in the brains of Tg2576 mice treated with 3mg/kg MRK-560 once a day for three months. Top shows representative western blot of three animals from vehicle- and MRK-560-treated groups revealing decrease in GFAP staining (arrow) indicative of reactive gliosis. Graph represents quantification of blots demonstrating significant reduction of GFAP in mice treated with MRK-560 vs. vehicle-treated animals (student's t-test, $p<0.05$) (n=14).

Figure 5. Chronic dosing of 3mg/kg MRK-560 once a day for three months does not induce abnormal changes in peripheral tissues of Tg2576 mice. Representative tissue sections from ileum (A, B), spleen (C, D) and thymus (E, F), demonstrating that treatment with MRK-560 (B, D, F) did not induce pathological changes in these tissues compared to the vehicle-treated group (A, C, E) despite lowering Aβ-containing plaques in the brain.

Figure 1

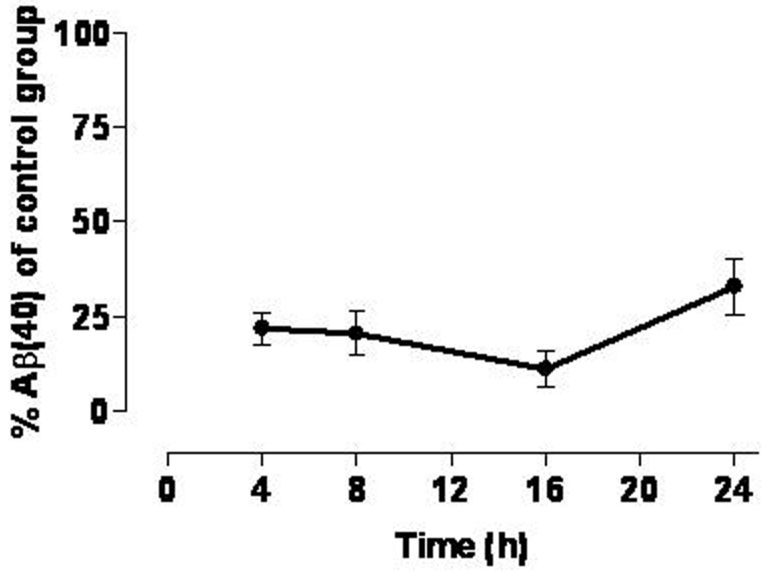

Figure 2

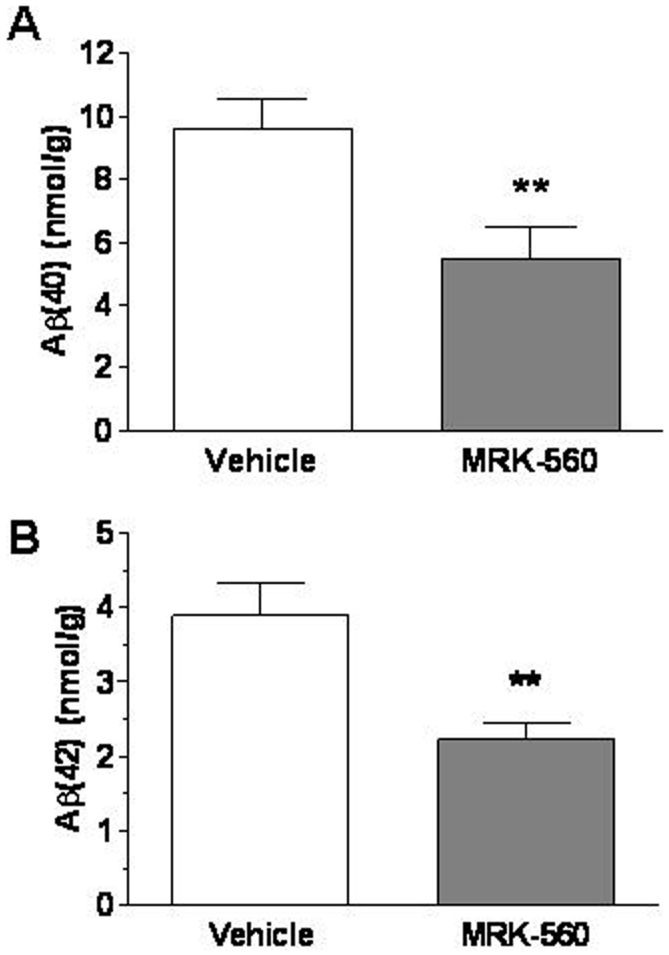
A
Aβ(40) (nmol/g)
12
10
8
6
4
2
0
**
Vehicle
MRK-560
B
Aβ(42) (nmol/g)
5
4
3
2
1
0
**
Vehicle
MRK-560

Figure 3

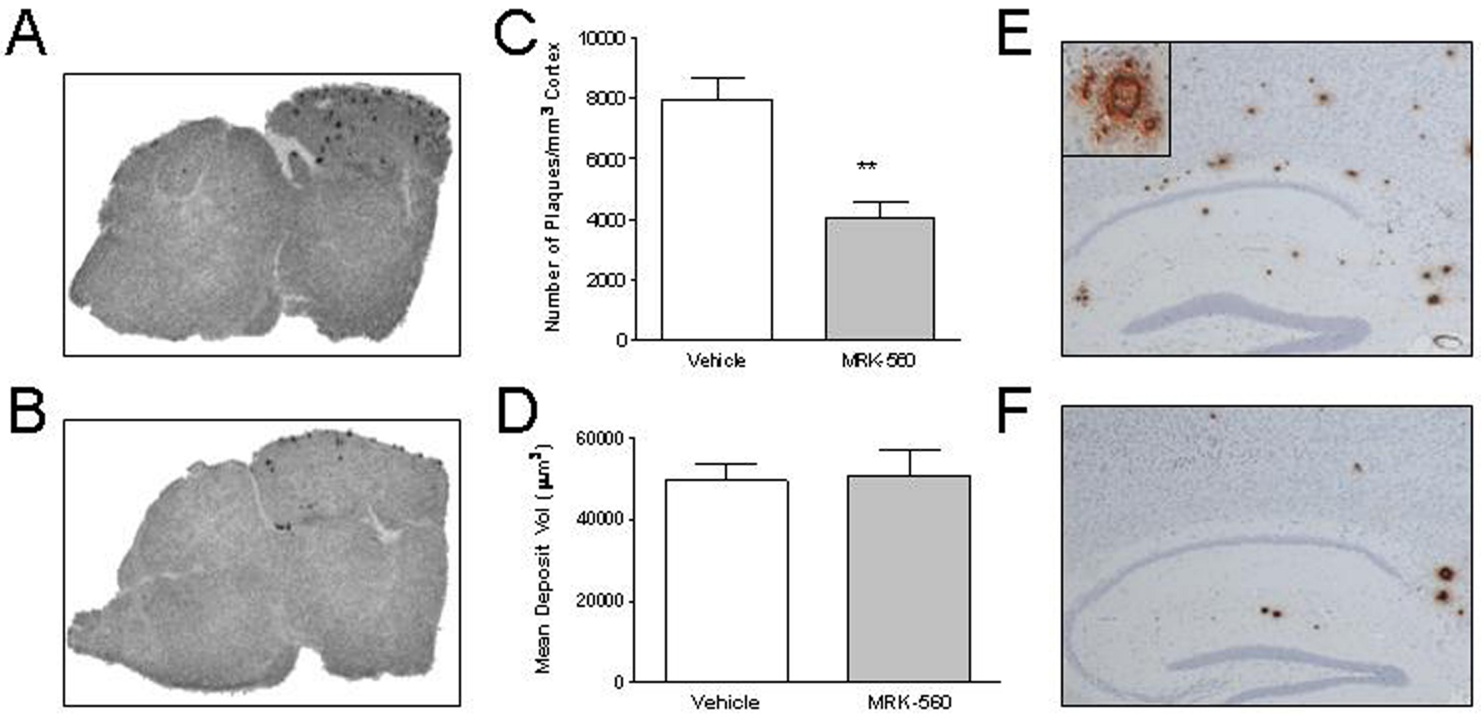
A
B
C
Number of Plaques/mm3 Cortex
10000
8000
6000
4000
2000
0
**
Vehicle
MRK-560
D
Mean Deposit Vol (µm3)
60000
40000
20000
0
Vehicle
MRK-560
E
F

Figure 4

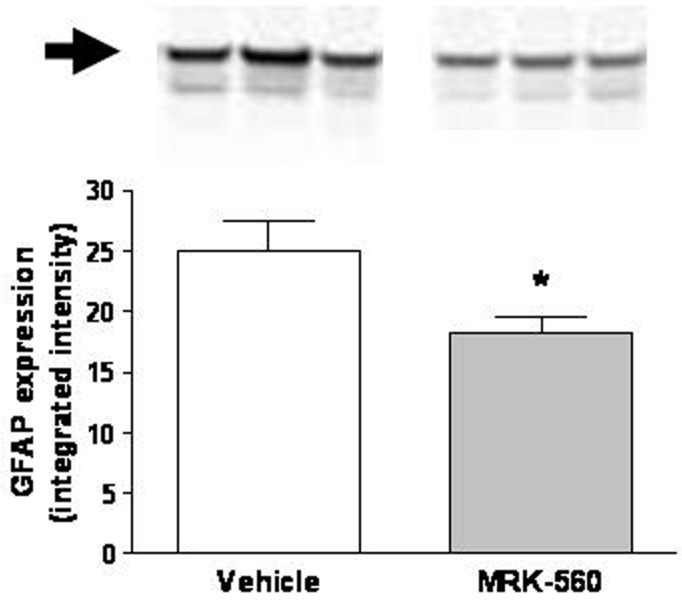
GFAP expression
(integrated intensity)
30
25
20
15
10
5
0
*
Vehicle
MRK-560

Figure 5